Molecular Therapy
Oncolytics
Original Article

Intraperitoneal oncolytic virotherapy for patients with malignant ascites: Characterization of clinical efficacy and antitumor immune response

Yalei Zhang,[1,2,3] Ling Qian,[1,2,3] Kun Chen,[1,2] Sijia Gu,[1,2] Jia Wang,[1,2] Zhiqiang Meng,[1,2] Ye Li,[1,2] and Peng Wang[1,2]

[1]Department of Integrative Oncology, Fudan University Shanghai Cancer Center, 270 Dong An Road, Shanghai 200032, China; [2]Department of Oncology, Shanghai Medical College, Fudan University, Shanghai 200032, China

Oncolytic viruses mediate antitumor responses through direct tumor cell lysis and induction of host antitumor immunity. However, the therapeutic efficacy of oncolytic viruses against malignant ascites has rarely been explored. This study aimed to evaluate the efficacy, safety, and immunomodulatory effect of an intraperitoneal injection of human type 5 recombinant adenovirus (called H101) against malignant ascites. Forty patients with malignant ascites were recruited and treated with intraperitoneal H101 in the Fudan University Shanghai Cancer Center. The 4-week clinical responses were determined by an objective assessment of ascites volume change. The ascites response rate and ascites control rate were 40% (16/40) and 75% (30/40), respectively. The major adverse events following intraperitoneal H101 administration were mild-to-moderate abdominal pain (8/40, 20.0%) and fever (11/40, 27.5%); no grade III/IV adverse events were observed. Mass cytometry and immunocytological analysis at baseline, and days 7 and 14 post-treatment showed that intraperitoneally injected H101 led to marked tumor cell depletion, increased dendritic cell and $CD8^+$ T cell densities. H101-meditated tumor-specific immune activation on day 14 post-treatment was further identified by enzyme-linked immunospot assay. In conclusion, intraperitoneal H101 administration was well tolerated and effective in treating malignant ascites; thus, its immune activation ability may be a promising tool in combination with immunotherapy.

INTRODUCTION

Malignant ascites (MA) is a common complication in late-stage malignancies that occurs as a consequence of peritoneal dissemination.[1] The presence of ascites has been associated with a decreased quality of life and poor survival (approximately 1–2 months).[2–5] To date, MA is still a critical problem, which lacks relevant clinical data and standard principles to guide clinical practice.[6]

Treatment options for MA mainly include intraperitoneal chemotherapy such as paclitaxel, S-1, and cisplatin; however, response to these treatments is achieved in only a small number of patients.[7–9] Molecular targeting therapy has emerged as another strategy to treat MA. Vascular endothelial growth factor (VEGF) blockade has achieved symptomatic relief of ascites volume in clinical studies based on the role of VEGF in promoting ascites production.[10–12] Catumaxomab, a chimeric antibody targeting CD3 and epithelial cell adhesion molecule (EPCAM), has been reported to improve the quality of life in patients with MA.[13] However, the risk of severe adverse effects, including fatal bowel perforation for the potent VEGF inhibitor aflibercept,[11,14] and hepatobiliary toxicity for catumaxomab, has limited the application of these treatments in patients with heavy disease burden.[15] Therefore, the identification of new treatment strategies against MA is critical.

Oncolytic viruses (OVs) are emerging therapeutic agents that can selectively target cancer cells and trigger immune activation. The application of OVs in combination with cancer immunotherapy in various solid tumors has become a promising therapeutic strategy.[16–18] Although extensive clinical data for OVs in treating solid tumors have been reported, studies on the therapeutic efficacy of OVs in treating MA are limited. The dense stroma and hypoxic microenvironment within a solid tumor mass limit the effectiveness of viral infection and intratumoral penetration of OVs.[19,20] In contrast, the microenvironment within MA may create a favorable condition for OV infection and OV-induced immune activation, indicating the feasibility of OVs to treat peritoneal malignancies and MA. A preclinical study reported that vesicular stomatitis virus, another type of OV, exerted a suppression effect on cancer cells from ascites and alleviated ascites accumulation in MA models.[21] Intraperitoneal administration of the oncolytic adenovirus OBP-401 demonstrated significant efficacy in treating peritoneal metastasis in a gastric cancer model.[22] A Phase I trial for the oncolytic vaccinia virus GL-ONC1 in patients with peritoneal carcinomatosis showed tolerability and efficient replication in cancer cells.[23]

Received 15 September 2021; accepted 13 March 2022;
https://doi.org/10.1016/j.omto.2022.03.003.

[3]These authors contributed equally

Correspondence: Peng Wang, MD, PhD, Department of Integrative Oncology, Fudan University Shanghai Cancer Center, 270 Dong An Road, Shanghai 200032, China.
E-mail: peng_wang@fudan.edu.cn
Correspondence: Ye Li, MD, PhD, Department of Integrative Oncology, Fudan University Shanghai Cancer Center, 270 Dong An Road, Shanghai 200032, China.
E-mail: li_ye@fudan.edu.cn

This is an open access article under the CC BY-NC-ND license (http://creativecommons.org/licenses/by-nc-nd/4.0/).

Table 1. Characteristics of patients with malignant ascites (n = 40)

Characteristics	N (%)
Gender	
Male	27 (67.5)
Female	13 (32.5)
Age, median (range), y	62 (32–84)
KPS score	
<80	0 (0)
≥80	40 (100)
Primary tumor type	
Pancreatic cancer	13 (32.5)
Hepatobiliary cancer	11 (27.5)
Gastrointestinal cancer	10 (25.0)
Other	6 (15.0)
Metastasis	
Liver	18 (45)
Peritoneum	27 (67.5)
Prior resection	
Yes	14 (35.0)
No	26 (65.0)
Ascites volume	
Small	1 (2.5)
Moderate	11 (27.5)
Massive	28 (70.0)
Line of previous chemotherapy	
1	11 (27.5)
2	3 (7.5)
3/4	26 (65.0)

KPS, Karnofsky performance status.

The human recombinant type 5 adenovirus H101 (also known as Oncorine) is an oncolytic adenovirus with specific genetic modifications.[24] The gene encoding the anti-apoptotic E1B55K protein that inactivates p53 was deleted, enabling selective replication only in cancer cells with aberrant p53 function, and a partial E3 region was also deleted to improve the safety of H101.[25] A Phase II clinical study of H101 in combination with chemotherapy showed promising antitumor ability and safety in patients with advanced cancer.[26] In 2004, a Phase III trial reported that compared with chemotherapy alone, H101 in combination with chemotherapy showed superior antitumor efficacy in 160 patients with head and neck or esophagus cancer.[27] H101 was subsequently approved by the Chinese Food and Drug Administration for treating nasopharyngeal carcinoma in combination with cisplatin, 5-fluorouracil, or both.[28] As the first OV agent applied in the clinic, H101 has been used in several malignancies for both clinical and experimental purposes.[29–31] In this study, we retrospectively evaluated the efficacy, safety, and immunomodulatory effect of intraperitoneal H101 against MA.

RESULTS

Patient characteristics

Forty patients who met the inclusion criteria were enrolled to evaluate the clinical efficacy of H101. The patient characteristics are listed in Table 1. The primary tumor types were pancreatic cancer (13/40), gastrointestinal cancer (10/40), and hepatobiliary cancer (11/40); other primary sites of tumors include ovary (2/40), prostate (1/40), lung (1/40), kidney (1/40), and cervix (1/40). The median age of the patients was 62 (32–84) years, and all of the patients showed a Karnofsky performance status score of ≥80. According to the ascites volume at baseline, 28 (70%) patients had a large amount of ascites (group +++), 11 (27.5%) patients had a medium amount of ascites (group ++), and only 1 (2.5%) patient had a small amount of ascites (group +). Among the 40 patients, 23 (57.5%) patients developed MA during chemotherapy. In addition, 18 (45%) patients were confirmed with liver metastasis, and 27 (67.5%) patients were confirmed with peritoneal metastasis by computed tomography (CT). Cytological identification of malignant cells from ascites fluid was positive in all of the patients. All of the patients experienced failure from chemotherapy treatment for MA. In the total patient group, 11 (27.5%) patients received first-line chemotherapy, 3 (7.5%) patients received second-line chemotherapy, and 26 patients (65%) received third- or fourth-line chemotherapy.

Efficacy and toxicity

Of the 40 patients with MA who received H101 injection, the disappearance of ascites was achieved in 5 (12.5%) patients, a decrease in ascites volume was observed in 11 (27.5%) patients, 14 (35%) patients showed no change in ascites volume, and 10 (25%) patients showed an increase in ascites volume, yielding an ascites response rate (ARR) of 40% and an ascites control rate (ACR) of 75%. Changes in ascites volume are shown in Figure 1A.

The treatment-related adverse events are listed in Table 2. No severe adverse events were reported. The major adverse events after the intraperitoneal injection of H101 were fever and abdominal pain. The temperature of 11 (27.5%) patients was >37°C. Seven (17.5%) patients reported mild to moderate abdominal pain and 1 (2.5%) patient reported severe abdominal pain. Elevated ALT was observed in 1 patient, and elevated Tbil was observed in 1 patient; 2 (5%) patients developed catheter-related infections. Other adverse events reported by patients included fatigue, chills, and digestive symptoms such as nausea, vomiting, constipation, and diarrhea; liver damage, hypotension, skin irritation, and myelosuppression were not observed. These adverse events only appeared within 24 h after H101 injection and were relieved after symptomatic treatment. There was no correlation between dose and response ($p = 0.2564$).

No correlation between preexisting anti-adenovirus neutralizing antibody and response

All six patients were determined to be positive (standard unit >11) for preexisting serum anti-adenovirus neutralizing antibody (immunoglobulin G [IgG]), as determined by ELISA (Figure 1B). The level of

A

Response	All patients (n=40)	Pancreatic cancer	Hepatobiliary cancer	Gastrointestinal cancer	Other
Disappeared	5 (12.5%)	0 (0%)	2 (18.2%)	3 (30%)	0 (0%)
Decreased	11 (27.5%)	5 (38.5%)	1 (9.1%)	4 (40%)	1 (16.7%)
No change	14 (35%)	3 (23.1%)	6 (54.5%)	2 (20%)	3 (50%)
Increase	10 (25%)	5 (38.5%)	2 (18.2%)	1 (10%)	2 (33.3%)
Ascites response	16 (40%)	5 (38.5%)	3 (27.3%)	7 (70%)	1 (16.7%)
Ascites control	30 (75%)	8 (61.5%)	9 (81.8%)	9 (90%)	4 (66.7%)

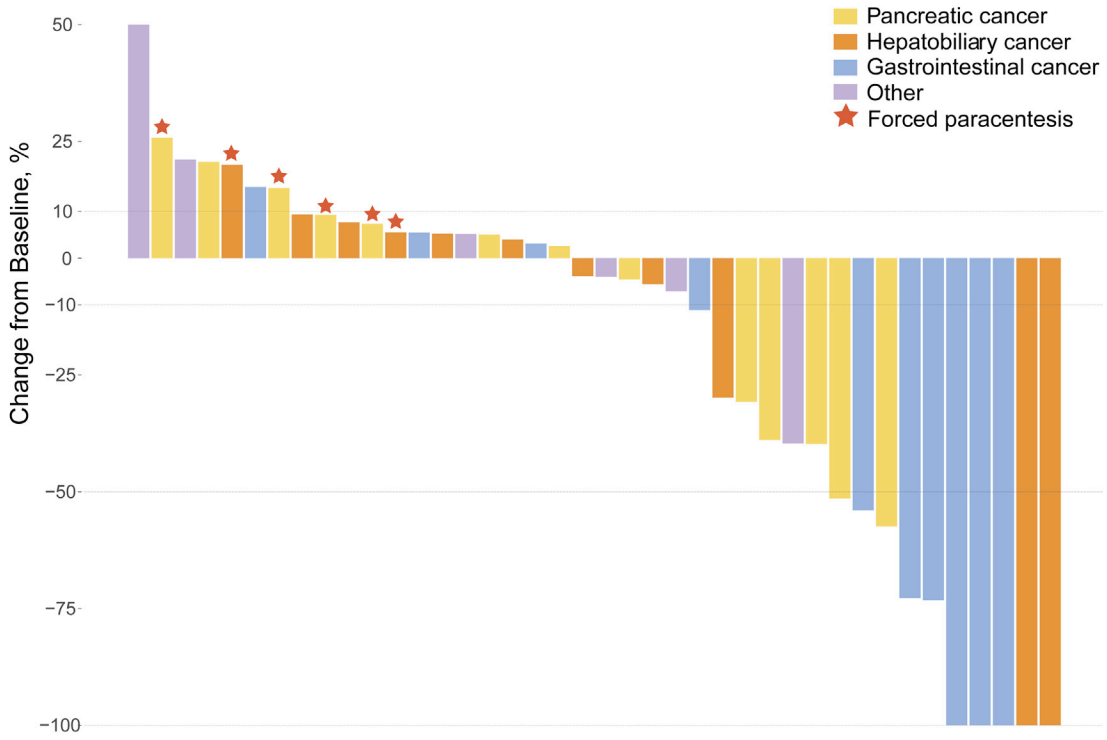

B

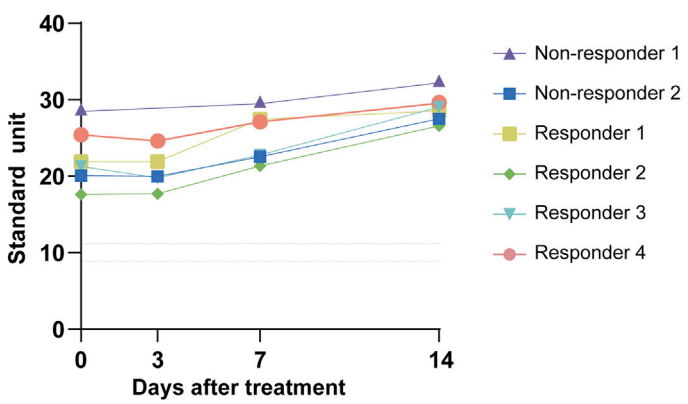

(legend on next page)

Table 2. Toxicity after H101 administration[a] (n = 40)

Adverse events	Any grade (%)	Grade 1–2 (%)	Grade 3 (%)	Grade 4 (%)
Systematic symptoms				
Fever	11 (27.5)	11 (27.5)	0 (0)	0 (0)
Fatigue	1 (2.5)	1 (2.5)	0 (0)	0 (0)
Chills	2 (5)	2 (5)	0 (0)	0 (0)
Hypotension	0 (0)	0 (0)	0 (0)	0 (0)
Skin irritation	0 (0)	0 (0)	0 (0)	0 (0)
Gastrointestinal disorders				
Abdominal pain	8 (20)	7 (17.5)	1 (2.5)	0 (0)
Vomiting	1 (2.5)	1 (2.5)	0 (0)	0 (0)
Nausea	2 (5)	2 (5)	0 (0)	0 (0)
Diarrhea	4 (10)	4 (10)	0 (0)	0 (0)
Constipation	1 (2.5)	1 (2.5)	0 (0)	0 (0)
Hematological disorders				
Anemia	0 (0)	0 (0)	0 (0)	0 (0)
Neutropenia	0 (0)	0 (0)	0 (0)	0 (0)
Leukopenia	0 (0)	0 (0)	0 (0)	0 (0)
Thrombocytopenia	0 (0)	0 (0)	0 (0)	0 (0)
Abnormal laboratory parameters				
ALT	1 (2.5)	1 (2.5)	0 (0)	0 (0)
AST	0 (0)	0 (0)	0 (0)	0 (0)
Tbil	1 (2.5)	1 (2.5)	0 (0)	0 (0)
Catheter-related infection	2 (5)	2 (5)	0 (0)	0 (0)

[a]Toxicities are reported following the Common Terminology Criteria for Adverse Events, version 4.

anti-adenovirus IgG was relatively stable on day 3, but then progressively increased on days 7 and 14 after H101 treatment. There is no correlation between the preexisting anti-adenovirus IgG level and response.

Mass cytometry (CyTOF) profiling revealed H101-induced intraperitoneal immune activation

T cell subsets were identified by the T cell marker CD3. The marker expression level of 20 $CD3^+$ T clusters is shown in a heatmap in Figure 2B. Based on the different expression levels of classical markers, 10 clusters of $CD4^+$ T cells, 8 clusters of $CD8^+$ T cells, 1 cluster of T regulatory (Treg) cells ($CD4^+$, $CD25^+$, and $CD127^{low}$), 1 cluster of $CD4^+$ $CD8^+$ double-positive (DP) cells, and 1 cluster of $CD4^-$ $CD8^-$ double-negative (DN) cells were identified (Figure 2B). The distribution of these main clusters and representative markers was visualized by t-distributed stochastic neighbor embedding (t-SNE) (Figure 2C). Further subclassification of specific phenotypes was performed according to marker expression. CD197 $(CCR7)^+$ and $CD45RA^-$ clusters were identified as central memory T cells (Tcm); exhausted T cells (Tex) were distinguished by $CD279^+$; $CD197^-$ and $CD45RA^-$ clusters were identified as effector memory T cells (Tem); and $CD197^-$ and $CD45RA^+$ clusters were identified as effector T cells (Teff). t-SNE plots of the normalized expression of representative markers were shown in Figure 2D. $CD4^+$ Tcm and $CD8^+$ Tem comprised the majority of $CD4^+$ T and $CD8^+$ T cells in MA samples (Figure 2E). DP and DN cells were not considered in the following analysis because their development and function have not been fully elucidated.[32,33]

Examination of the dynamic changes in T cell subsets showed that the percentage of $CD8^+$ T cells ($CD8^+$ Tem, specifically) markedly increased at day 14 compared with baseline (Figure 2E). Expression of CD8A on days 7 and 14 after H101 injection increased in responders compared with non-responders (Figure 2F). An increased fraction of $CD8^+$ T cells was observed in 3 out of 4 responders on day 14 after H101 injection, while in non-responders, the dynamic fraction of $CD8^+$ T cell remains stable (Figure 2G). The dynamic t-SNE plot of the exhaustion marker PD-1 (CD279) expression between responders and non-responders is shown in Figure 2H; the expression of PD1 was increased on day 7 after H101 injection and slightly dropped on day 14 after H101 injection in both responders and non-responders, but this change was more evident in responders. The dynamic change in the fraction of $PD1^+$ cells was observed on day 7 after H101 injection, and 3 out of 4 responders showed an increase in the fraction of $PD1^+$ cells at different time points (Figure 2I). Increased PD1 expression on day 7 after H101 injection was shown in Treg and $CD4^+$ Tex cells (Figure 2J), suggesting the exhausted and dysfunctional phenotype induced by H101. The percentages of T cell subtypes in 6 patients on days 0, 7, and 14 after H101 injection are shown in Figure 2K.

In the non-T cell panel, based on the expression level of classical markers in Figure 3A, 20 $CD3^-$ clusters were classified into 3 clusters of dendritic cells (DCs) (human leukocyte antigen-DR isotype [$HLADR^+$] and $CD123^+/CD11c^+$), 5 clusters of macrophages (Macros) ($CD68^+$), 6 clusters of myeloid suppressor cells (MDSCs) ($HLADR^{low}$ and $CD11b^+$), 5 clusters of monocytes ($CD14^{high}$), and 1 cluster of B cells ($CD20^+$). The phenotypically distinct subpopulations were further defined as $CD16^-$ (non-classic) monocytes, $CD16^+$ (classic) monocytes, $HLADR^+$ macrophages, $CD38^-$ MDSCs, $CD123^+$ DCs (pDCs), $CD11c^+$ DCs (mDCs), and B cells.

Figure 1. Clinical efficiency of H101 injection for treatment of malignant ascites (MA)

(A) The ARR and ACR after H101 administration of 40 patients with different types of cancer (top). The change in ascites volume between day 0 (baseline) and day 28 after H101 treatment (bottom). (B) Serum anti-adenovirus IgG level in 6 patients on days 0, 3, 7, and 14 after H101 treatment, as measured by ELISA. Levels of >11 standard units indicate positive results, levels of <9 standard units indicate negative results, and levels of 9–11 standard units indicate inconclusive results. No blood sample was collected from non-responder #1 on day 3 after H101 treatment.

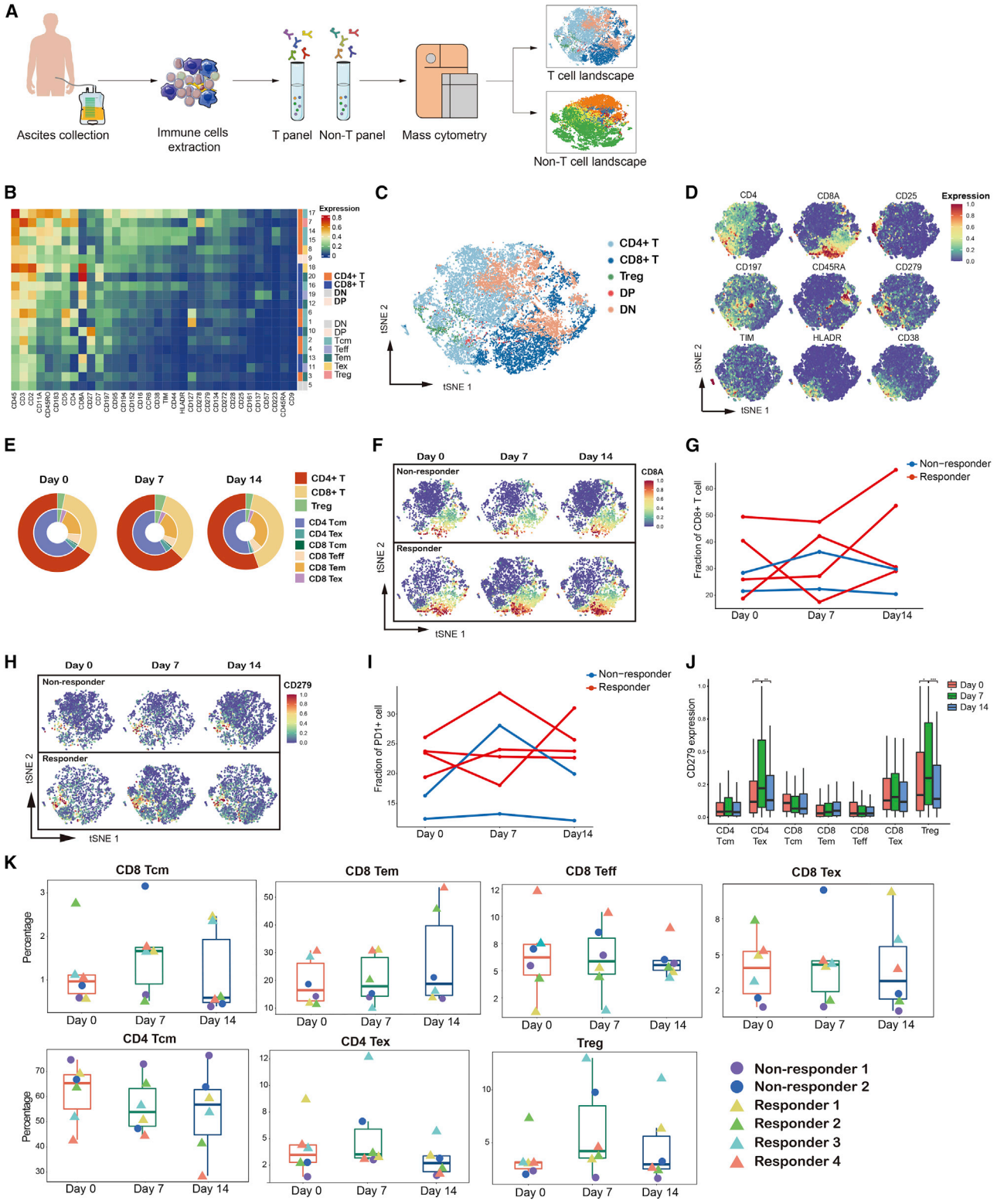

(legend on next page)

The distribution of these five main clusters was visualized by t-SNE plot (Figure 3B). t-SNE plots of the normalized expression of representative markers are shown in Figure 3C. $CD38^-$ MDSC cells and monocytes comprise approximately 50% and 25% of myeloid cells, respectively, in MA samples. Antitumorigenic ($CD68^+$ $HLADR^+$) macrophages were also a major component in MA samples (Figure 3D). Increased DC and slightly decreased monocyte fractions were observed on day 7 after H101 injection; other cell components remained relatively stable during treatment (Figure 3D). Two responders showed increases in DC fractions on day 7 after H101 injection (Figure 3E). No evident increase was observed in programmed death-ligand 1 (PD-L1) (CD274) expression in non-responders compared with responders, due to the limited number of cells (Figure 3F). The fraction of $PD\text{-}L1^+$ myeloid cells increased in 3 out of 4 responders and slightly decreased in non-responders on day 14 after H101 injection (Figure 3G). PD-L1 expression was increased in all of the myeloid subtypes, except for $CD38^-$ MDSCs, and increased expression was especially observed in $CD16^-$ mono, $CD11c^+$ DCs, and $CD123^+$ DCs (Figure 3H). The change in percentages of 8 non-T cell subtypes on days 0, 7, and 14 after H101 injection is shown in Figure 3I.

Tumor cell depletion and increased immune infiltration induced by intraperitoneal H101 injection

To further explore the oncolytic and antitumor effect of H101, immunocytochemistry (ICC) staining was performed in samples from the same six patients. Representative images of MA sections are shown in Figure 4. Anticytokeratin (CK) staining of MA sample sections reveals that tumor cells made up only a small portion of the MA samples. A significant decrease in the density of tumor cells and a significant increase in the density of $CD8^+$ T cells were separately observed in the ascites samples at day 7 and day 14 after H101 injection, as compared with at baseline ($p < 0.05$) (Figure 4A). In the staining for viral protein E1A, $E1A^+$ virus-infected cells were observed in 3 out of the 6 patients at day 7 after H101 injection ($1.16\% \pm 1.87\%$), whereas at day 14 after H101 treatment, the viral proteins were rarely detected in any of the patients (Figures 4B and S1).

H101 triggered tumor-specific immune activation in patients with MA

To further identify whether the immune response triggered by H101 was tumor specific, we collected ascites samples from one additional patient on days 0, 7, and 14 after H101 treatment and analyzed the tumor-specific $CD8^+$ T cells by using an interferon- γ (IFN-γ) enzyme-linked immunospot (ELISpot) assay with or without tumor-containing lysate. Compared with the number at baseline, the number of IFN-γ^+ spots generated from $CD8^+$ T cells on day 14 after H101 treatment showed an increasing trend, indicating a tumor-specific immune response is likely activated by H101 (Figure 4C).

DISCUSSION

This is the first study to evaluate the antitumor efficacy and immune response of an OV in treating MA. As an intractable complication of advanced malignancies, MA severely decreases the quality of life and correlates closely with a poor response rate to chemotherapy.[34] In this study, H101 achieved a higher ACR and exerted more durable efficacy as compared with symptomatic treatments, such as diuretics.[35] Although an assessment of the patient quality of life was not included in the present analysis owing to the retrospective nature of the study, quality of life has been shown to correlate with ascites volume.[36] In addition, an intraperitoneal injection of H101 was well tolerated with manageable toxicity; therefore, H101 provides a valid option for cancer patients in the advanced stage of the disease with a poor general condition, including patients with MA.

All six patients were found to be positive for preexisting anti-adenovirus IgG; this finding is in agreement with the high seroprevalence of neutralizing antibody against human adenovirus serotype-5 in cancer patients that has been reported previously.[37] E1A staining showed that virus infection was observed in only 3 out of 6 patients on day 7 after H101 treatment and was rarely detected on day 14 after H101 treatment, while the serum level of antiadenovirus IgG kept increasing, indicating an existing antiviral immune response. The elimination of virus-infected cells on day 14 after H101 treatment shown by E1A staining may be a consequence of the eradication of tumor cells. Therefore, to explore the dynamic viral infection status, future studies should constantly monitor the viral load of H101 and the neutralizing antibody level by applying more accurate methods, such as qPCR and virus titration, throughout the entire evaluation period.

As an emerging candidate for cancer treatment, OVs have been shown to not only specifically lyse the tumor cell population but also promote immunogenic cell death and modulate the tumor immune microenvironment, which favors the intratumoral infiltration of T cells and brings improved clinical efficacy.[16,38] In this study, the dynamic immune landscape of MA during intraperitoneal oncolytic virotherapy was revealed. As a prerequisite target in the immune

Figure 2. Dynamic T cell landscape of MA during intraperitoneal H101 treatment (n = 6)

(A) Overview of MA sample collection and processing for CyTOF. (B) Heatmap of normalized T cell marker expression for 20 clusters. (C) A t-SNE plot demonstrating 36,000 $CD3^+$ T cells from MA samples, colored by T cell subtype. (D) t-SNE plots of normalized marker expression for the classification of 36,000 T cells from all of the samples. (E) Pie charts representing the relative frequencies of T-cell types on days 0, 7, and 14 after H101 treatment. (F) t-SNE plots of normalized CD8A expression in responders (n = 4) and non-responders (n = 2) on days 0, 7, and 14 after H101 treatment. (G) Dynamic fraction of $CD8^+$ T cells in responders and non-responders on days 0, 7, and 14 after H101 treatment. (H) t-SNE plots of normalized CD279 (PD1) expression in responders and non-responders on days 0, 7, and 14 after H101 treatment. (I) Dynamic fraction of $PD1^+$ cells in responders and non-responders on days 0, 7, and 14 after H101 treatment. (J) Normalized CD279 expression in specific T cell subtypes on days 0, 7, and 14 after H101 treatment. (K) Dynamic fraction of 7 T cell subtypes ($CD8^+$ Tcm, $CD8^+$ Tem, $CD8^+$ Teff, $CD8^+$ Tex, $CD4^+$ Tcm, $CD4^+$ Tex, and Treg) in responders and non-responders on days 0, 7, and 14 after H101 treatment.

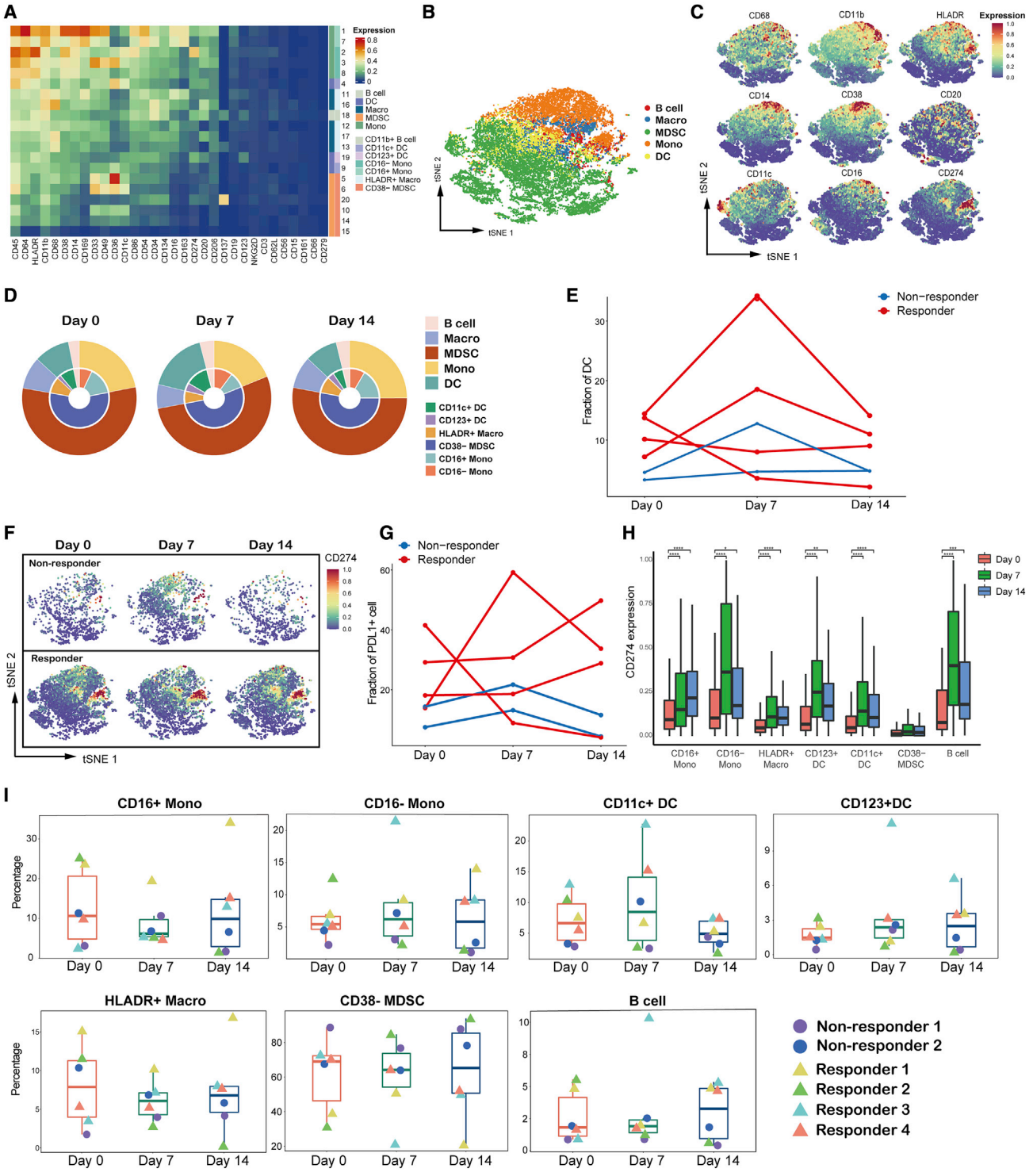

Figure 3. Dynamic non-T cell landscape of MA during intraperitoneal H101 treatment (n = 6)

(A) Heatmap of normalized non-T cell marker expression for 20 clusters. (B) A t-SNE plot demonstrating 36,000 CD3^{-} non-T cells from MA samples, colored by non-T cell subtypes. (C) t-SNE plots of normalized marker expression for the classification of 36,000 non-T cells from all samples. (D) Pie charts representing the relative frequencies of non-T cell types on days 0, 7, and 14 after H101 treatment. (E) Dynamic fraction of DCs in responders and non-responders on days 0, 7, and 14 after H101 treatment.

(legend continued on next page)

cycle, the observed increase in the number of DCs suggests the enhanced exposure and presentation of antigen induced by oncolysis, and the relative augmentation of $CD8^+$ T cells indicates activation of the antitumor immune cycle. We also observed an acquired immune resistance characterized by elevated PD1/L1 expression on immune cells in response to the antitumor inflammatory response. This resistance was more evident in responders, re-confirming the immunomodulatory effect of intraperitoneal H101 in addition to oncolysis. Our data show that PD1 expression was upregulated in Tregs, which has also been reported during chronic viral infection, and use of a PD1 blockade could shift Tregs into a more exhausted state.[39,40] $PD\text{-}L1^+$ tumor-associated myeloid cells have been reported to be associated with clinical outcomes because they lead to T cell exhaustion via the PD1/L1 axis.[41,42] Our data indicating that PD-L1 expression was upregulated at day 7 after H101 treatment show that most myeloid cells in MA are shifted toward a pro-tumorigenic phenotype after H101 injection. According to our CyTOF, ICC, and ELISpot results, the $PD1/L1^+$ tumor microenvironment with increased tumor-specific $CD8^+$ T cell infiltration created by H101 treatment provides a target for immune checkpoint blockade therapy, indicating the clinical practicability of intraperitoneal virotherapy in combination with immunotherapy.

This study has several limitations. This was a single-center retrospective study, which carries limitations in the study design and data collection. We focused on the short-term clinical efficacy of H101 (within 4 weeks of injection), and patients with MA received H101 administration for only one cycle, with a fixed dose according to the ascites volume. Therefore, the optimal treatment design of intraperitoneal H101 treatment, including the dosage and delivery cycle, need to be clarified. In addition, virus-induced immune activation revealed by CyTOF, cytological, and ELISPOT analysis was not able to fully account for the virus-mediated efficacy because of the limited sample size. Expansion in sample size will be considered in a subsequent clinical trial. Finally, whether H101 could bring long-term clinical benefits against MA and whether the efficacy and toxicity of H101 are dose dependent remain to be explored in future studies. We have launched a prospective clinical trial of H101 against refractory MA (NCT04771676), and the efficacy, toxicity, and immunomodulatory effects of intraperitoneal H101 will be comprehensively evaluated.

In conclusion, despite the acknowledged limitations due to the nature of retrospective studies, we observed encouraging clinical benefits, manageable toxicity, and solid evidence of the immune activation of H101 against MA. Considering the poor prognosis of patients with peritoneal metastasis and MA, our clinical outcomes are promising. Further studies to optimize the treatment regimens and assess the contribution of H101 in combination with immunotherapies in anticancer treatment are warranted.

MATERIALS AND METHODS

Patients

This study was approved by the ethics committee of the Fudan University Shanghai Cancer Center (Shanghai, China), and written informed consent was obtained from all of the patients before their entry into the study. Clinical records of 45 patients with MA who received intraperitoneal administration of H101 at Fudan University Shanghai Cancer Center from January 2016 to December 2016 were retrospectively reviewed. The inclusion criteria of patients included the following: (1) histologically or cytologically diagnosed solid tumor malignancy, (2) malignant peritoneal effusion and ascites detected by ultrasonography or CT and confirmed by cytologic examination of intraperitoneal exfoliated tumor cells; (3) failed response to chemotherapy against MA; and (4) Karnofsky performance status (KPS) ≥ 60. Patients with a history of applying diuretics and paracentesis were allowed to enter the study. The exclusion criteria included the following: (1) previous (<28 days) or concurrent treatment with systemic or intraperitoneal chemotherapy or biological agents such as monoclonal antibodies; (2) previous treatment of immunoregulatory agents such as intraperitoneal injection of bacillus Calmette-Guerin; and (3) concurrent severe illness such as active infection, psychiatric illness, serious heart disease, poorly controlled hypertension or diabetes mellitus that would limit safety and compliance with study requirements. Based on these criteria, a total of 40 patients were enrolled for analysis.

To perform CyTOF and ICC, 500–1,000 mL ascites were collected at baseline (day 0) before ultrasonic determination, and 200 mL ascites were collected on days 7 and 14 after H101 treatment from 6 of the 40 patients. Blood samples of the same six patients were also collected to detect serum antiadenovirus neutralizing antibody on days 0, 3, 7, and 14 after H101 treatment. In addition, to identify tumor-specific $CD8^+$ T cell response, ascites collection from 1 additional patient was conducted on days 0 and 14 for ELISpot assay.

Treatment

Each vial of H101 (−20°C, Shanghai Sunway Biotech, Shanghai, China) contained 0.5 mL sterile viral solution with 5.0×10^{11} viral particles (vp) and titered at a median tissue culture infective dose ($TCID_{50}$) <1:60. To achieve symptomatic relief and acquire ascites cells, 500–1,000 mL peritoneal effusion was drained by placing the peritoneal drainage catheter at the left or right lower quadrant of the abdomen. Then, ultrasonic measurement was performed to acquire the ascites volume at baseline. H101 diluted in 5 mL 0.9% sodium chloride solution was then intraperitoneally injected through the drainage catheter. The injection dose of H101 was determined by the ascites volume: 5.0×10^{11} vp for a small amount, 1×10^{12}–1.5×10^{12} vp for a medium amount, and 2×10^{12} vp for a massive amount (classification of the ascites amount is described

(F) t-SNE plots of normalized CD274 (PD-L1) expression in responders and non-responders on days 0, 7, and 14 after H101 treatment. (G) Dynamic fraction of $PD\text{-}L1^+$ cell in responders and non-responders on days 0, 7, and 14 after H101 treatment. (H) Normalized CD274 expression in specific non-T cell subtypes on days 0, 7, and 14 after H101 treatment. (I) Dynamic fraction of 7 non-T cell subtypes ($CD16^+$ mono, $CD16^-$ mono, $CD11c^+$ DCs, $CD123^+$ DCs, $HLADR^+$ Macros, $CD38^-$ MDSCs, B cells) in responders and non-responders on days 0, 7, and 14 after H101 treatment.

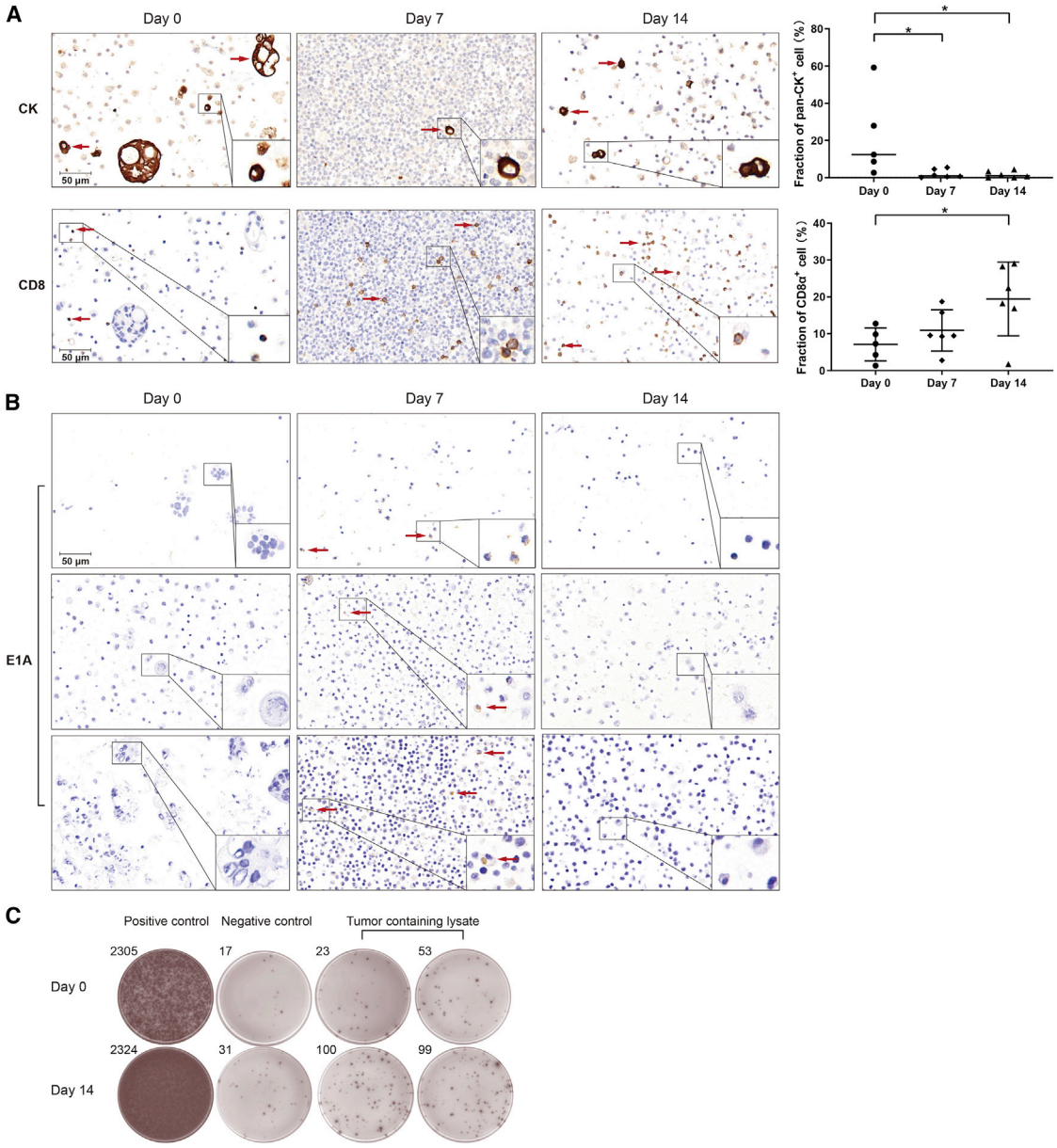

Figure 4. Tumor cell depletion and antitumor immune activation induced by H101

(A) Representative image of MA samples at baseline (day 0) and day 7 and day 14 after H101 injection. Expressions of pan-CK$^+$ tumor cells and CD8$^+$ T cells were determined by ICC. Dynamic change in the proportions of tumor cells and CD8$^+$ T cells at baseline and days 7,14 after H101 treatment (n = 6). The ascites sample from 1 patient on day 0 was not able to be calculated because few ascites cells were collected for formalin fixation. (B) Representative viral protein E1A staining on days 0, 7, and 14 after H101 injection in 3 patients. The formation of inclusion bodies due to viral infection was observed in 1 of these 3 patients (bottom). (C) The CD8$^+$ T cell response against tumor-containing lysate on days 0 and 14 after H101 injection in 1 responder was assessed using IFN-γ enzyme-linked immunospot (ELISpot). The number of spots in each well is listed above the well.

in the following section). For patients who received the maximal dose (2×10^{12} vp), 1×10^{12} vp of H101 was injected twice, 1 day apart. Immediately after H101 injection, patients were instructed to change position every 5 min over a 30-min period to achieve an equal distribution of H101 throughout the peritoneal cavity. A second paracentesis was performed if patients required relief of ascites symptoms within 4 weeks from MA progression (forced paracentesis).

Response evaluation

The response after 28 days was evaluated by the objective assessment of ascites volume using transabdominal ultrasonography. An

ultrasound position-setting measurement was performed at baseline and day 28 after H101 injection to measure the change in ascites volume. Briefly, patients were maintained in a supine position, and a 3- to 5-MHz linear or a 3- to 5-MHz convex-array transducer was used to perform the ultrasound scan. The depth of the largest free fluid pocket at four abdominal quadrants, including both inguinal regions and perihepatic and perisplenic regions, was measured in a horizontal plane. The maximal value of the depth measured at the four positions was used to determine the ascites volume.[43] To achieve an objective assessment of ascites volume, ultrasonography was performed by an experienced ultrasound technician who was blinded to the study design. The ascites volume was classified into three categories according to the maximal depth measured by ultrasonography: small amount (+, maximal depth <30 mm), medium amount (++, 30 mm $\geq$ maximal depth <60 mm), and massive amount (+++, maximal depth $\geq$60 mm). The treatment outcomes were divided into the following four categories, as described in a previous report: disappeared: complete disappearance of ascites at day 28 after H101 injection; decreased: >10% reduction of ascites volume after H101 injection compared with baseline; no change: decrease or increase of ascites volume within 10% compared with baseline; and increased: >10% increase of ascites volume compared with baseline.[44] Patients who received a second paracentesis to relieve ascites-related symptoms within 4 weeks from MA progression (forced paracentesis) were determined to be increased regardless of the change in ascites volume. Responders and non-responders were separately defined as patients with disappeared or decreased ascites and patients who showed no reduction in ascites volume.

Toxicity

Patients were required to be hospitalized for 24 h after H101 injection, and a 4-week follow-up was conducted to monitor treatment-related adverse events. Toxicity was graded according to the Common Terminology Criteria for Adverse Events of the National Cancer Institute, version 4.0.

CyTOF analysis of peritoneal immune activation

Ascites samples of 6 patients were collected at baseline (day 0) and 7 and 14 days after H101 treatment for CyTOF analysis. Briefly, ascites fluid was collected and centrifuged at 1,500 rpm for 5 min to obtain ascites cells. The cell pellet was re-suspended in 3× volume of phosphate-buffered saline (PBS) and filtrated with a 100-μm cell strainer. After centrifugation and red cell lysis, cells were re-suspended with Hank's solution and added onto an equal volume of Ficoll solution for gradient centrifugation. The white layer of immune cells at the interface was collected and washed twice with staining buffer. A total of 34 and 32 cell-surface antibodies of T and non-T panel (Fluidigm, South San Francisco, CA, USA) (Table S1) were mixed in a 100-μL volume of Maxpar Cell Staining Buffer. Up to 3 million cells per sample were stained with antibody mixer (see supplemental information). After washing with 1 mL Maxpar Cell Staining Buffer, cells were re-suspended in 2 mL cell intercalation solution (125 nM Cell-ID Intercalator-Ir in Maxpar Fix and Perm Buffer). Analysis with the CyTOF 2 Mass Cytometer was subsequently performed. Initial data processing was conducted using Cytobank (https://premium.cytobank.org/cytobank/), and subsequent analysis including dimensional reduction, clustering analysis was performed using R packages FlowSOM, cytoCore, and Rtsne.

Immunocytochemistry of ascites cells

Cells collected from ascites samples at baseline and 7 and 14 days after H101 injection were fixed and embedded. The cells were separately stained with anti-CD8α monoclonal antibody (mAb) (ab237709, Abcam, Cambridge, UK), anti-pan-CK mAb (ab7753, Abcam), and anti-Ad5 E1A mAb (MA5-13643, Thermo Fisher Scientific, Fremont, CA, USA). Five high-power fields (40×) were randomly selected and the numbers of positive cells and total cells were assessed and calculated by a professional pathologist (J.F.), who was unaware of the grouping. The proportion of positive cells in each slide was calculated as positive cell number/total cell number. The proportions of the different fields of each sample were averaged for statistical analysis.

ELISpot identification of tumor-specific $CD8^+$ T cells

Ascites cells were collected from one additional patient who was defined as a responder. $CD45^-$ cells were sorted from ascites cells collected at baseline using $CD45^-$-specific magnetic-activated cell sorting (MACS) beads (cat. no. 130-045-801, Miltenyi Biotec, Bergisch Gladbach, Germany) and were lysed via three freeze-and-thaw cycles to make a tumor-containing lysate. The $CD8^+$ T cells were then isolated using CD8-specific MACS beads (cat. no. 130-045-201, Miltenyi Biotec). Sorted $CD8^+$ T cells were plated in duplicate wells of an IFN-γ ELISpot (1×10^5 cells/well) and stimulated with tumor-containing lysate (25 μg/mL) collected at baseline for 24 h. Spot formation was performed in accordance with the manufacturer's instructions (cat. no. 2110002, Dakewe Biotech, Beijing, China). Plates were read and analyzed using a Mabtech ASTOR ELISpot Reader (Mabtech AB, Stockholm, Sweden).

Detection of antiadenovirus neutralizing antibody by ELISA

The levels of antiadenovirus neutralizing antibody in serum samples taken from 6 patients on days 0, 3, 7, and 14 after H101 treatment were measured using an anti-Adenovirus IgG human ELISA kit (Abcam, ab108705). Adenovirus IgG positive, negative, and cutoff controls and prediluted serum samples were added into triplicate wells of a 96-well plate that had been pre-coated with adenovirus antigen. After washing, horseradish peroxidase-labeled anti-human IgG conjugate and 3,3′, 5,5' tetramethylbenzidine dihydrochloride (TMB) substrate were added in accordance with the manufacturer's instructions. Finally, the absorbance at 450 nm was read on a Bio-Rad Model 550 microplate reader (Bio-Rad, Hercules, CA, USA). Samples are considered positive or negative if the absorbance value is greater or lower, respectively, than 10% over the cutoff value. The results are shown using standard units, which equals the (patient [mean] absorbance value × 10)/cutoff value. A standard unit of 10 was set as the cutoff value; values of <9, >10, or 9–11 represent negative, positive, or inconclusive results, respectively.

Statistical analysis

Statistical analyses were performed using GraphPad Prism 8 (GraphPad, San Jose, CA, USA) software. The ARR was calculated as the ratio of the sum of patients with disappeared and decreased ascites to the total number of patients, which equals (disappeared + decreased)/total. The ACR was determined as the ratio of patients who showed no progression of ascites volume, which equals (disappeared + decreased + no change)/total. Data are expressed as means ± standard deviations (SDs). The correlation between dose and response was calculated by the chi-square test. All of the statistical tests were two sided. Differences between groups were analyzed by one-way ANOVA. $p < 0.05$ was considered significant.

SUPPLEMENTAL INFORMATION

Supplemental information can be found online at https://doi.org/10.1016/j.omto.2022.03.003.

ACKNOWLEDGMENTS

This work was financially supported by the National Natural Science Foundation of China (82025035 and 81871989); the Shanghai Science and Technology Committee Program (19XD1420900), and the Shanghai Education Commission Program (17SG04). The graphical abstract was created with BioRender.com.

AUTHOR CONTRIBUTIONS

The concept of this study was developed by P.W. and Y.L. Clinical records analyses, clinical sample processing, and manuscript drafting were conducted by Y.Z., L.Q., K.C., and S.G. Suggestions for revision were provided by P.W. and Z.M.

DECLARATION OF INTERESTS

The authors declare no competing interests.

REFERENCES

1. Cavazzoni, E., Bugiantella, W., Graziosi, L., Franceschini, M.S., and Donini, A. (2013). Malignant ascites: pathophysiology and treatment. Int. J. Clin. Oncol. *18*, 1–9.
2. Chau, I., Norman, A.R., Cunningham, D., Waters, J.S., Oates, J., and Ross, P.J. (2004). Multivariate prognostic factor analysis in locally advanced and metastatic esophagogastric cancer–pooled analysis from three multicenter, randomized, controlled trials using individual patient data. J. Clin. Oncol. *22*, 2395–2403.
3. Iwasa, S., Nakajima, T.E., Nakamura, K., Takashima, A., Kato, K., Hamaguchi, T., Yamada, Y., and Shimada, Y. (2012). First-line fluorouracil-based chemotherapy for patients with severe peritoneal disseminated gastric cancer. Gastric cancer *15*, 21–26.
4. Takahara, N., Isayama, H., Nakai, Y., Sasaki, T., Saito, K., Hamada, T., Mizuno, S., Miyabayashi, K., Mohri, D., Kogure, H., et al. (2015). Pancreatic cancer with malignant ascites: clinical features and outcomes. Pancreas *44*, 380–385.
5. Koo, D.H., Ryoo, B.Y., Kim, H.J., Ryu, M.H., Lee, S.S., Moon, J.H., Chang, H.M., Lee, J.L., Kim, T.W., and Kang, Y.K. (2011). A prognostic model in patients who receive chemotherapy for metastatic or recurrent gastric cancer: validation and comparison with previous models. Cancer Chemother. Pharmacol. *68*, 913–921.
6. Maeda, H., Kobayashi, M., and Sakamoto, J. (2015). Evaluation and treatment of malignant ascites secondary to gastric cancer. World J. Gastroenterol. *21*, 10936–10947.
7. Shukuya, T., Yasui, H., Boku, N., Onozawa, Y., Fukutomi, A., Yamazaki, K., Taku, K., Kojima, T., and Machida, N. (2010). Weekly Paclitaxel after failure of gemcitabine in pancreatic cancer patients with malignant ascites: a retrospective study. Jpn. J. Clin. Oncol. *40*, 1135–1138.
8. Zhao, H., Li, X., Chen, D., Cai, J., Fu, Y., Kang, H., Gao, J., Gao, K., and Du, N. (2015). Intraperitoneal administration of cisplatin plus bevacizumab for the management of malignant ascites in ovarian epithelial cancer: results of a phase III clinical trial. Med. Oncol. *32*, 292.
9. Takahara, N., Isayama, H., Nakai, Y., Ishigami, H., Satoi, S., Mizuno, S., Kogure, H., Matsubara, S., Yamamoto, N., Yamaguchi, H., et al. (2016). Intravenous and intraperitoneal paclitaxel with S-1 for treatment of refractory pancreatic cancer with malignant ascites. Invest. New Drugs *34*, 636–642.
10. Numnum, T.M., Rocconi, R.P., Whitworth, J., and Barnes, M.N. (2006). The use of bevacizumab to palliate symptomatic ascites in patients with refractory ovarian carcinoma. Gynecol. Oncol. *102*, 425–428.
11. Colombo, N., Mangili, G., Mammoliti, S., Kalling, M., Tholander, B., Sternas, L., Buzenet, G., and Chamberlain, D. (2012). A phase II study of aflibercept in patients with advanced epithelial ovarian cancer and symptomatic malignant ascites. Gynecol. Oncol. *125*, 42–47.
12. Mulder, S.F., Boers-Sonderen, M.J., van der Heijden, H.F., Vissers, K.C., Punt, C.J., and van Herpen, C.M. (2014). A phase II study of cediranib as palliative treatment in patients with symptomatic malignant ascites or pleural effusion. Target Oncol. *9*, 331–338.
13. Wimberger, P., Gilet, H., Gonschior, A.K., Heiss, M.M., Moehler, M., Oskay-Oezcelik, G., Al-Batran, S.E., Schmalfeldt, B., Schmittel, A., Schulze, E., and Parsons, S.L. (2012). Deterioration in quality of life (QoL) in patients with malignant ascites: results from a phase II/III study comparing paracentesis plus catumaxomab with paracentesis alone. Ann. Oncol. *23*, 1979–1985.
14. Gotlieb, W.H., Amant, F., Advani, S., Goswami, C., Hirte, H., Provencher, D., Somani, N., Yamada, S.D., Tamby, J.F., and Vergote, I. (2012). Intravenous aflibercept for treatment of recurrent symptomatic malignant ascites in patients with advanced ovarian cancer: a phase 2, randomised, double-blind, placebo-controlled study. Lancet Oncol. *13*, 154–162.
15. Sebastian, M., Passlick, B., Friccius-Quecke, H., Jager, M., Lindhofer, H., Kanniess, F., Wiewrodt, R., Thiel, E., Buhl, R., and Schmittel, A. (2007). Treatment of non-small cell lung cancer patients with the trifunctional monoclonal antibody catumaxomab (anti-EpCAM x anti-CD3): a phase I study. Cancer Immunol. Immunother. *56*, 1637–1644.
16. Ribas, A., Dummer, R., Puzanov, I., VanderWalde, A., Andtbacka, R.H.I., Michielin, O., Olszanski, A.J., Malvehy, J., Cebon, J., Fernandez, E., et al. (2017). Oncolytic virotherapy promotes intratumoral T cell infiltration and improves anti-PD-1 immunotherapy. Cell *170*, 1109–1119.e10.
17. Andtbacka, R.H., Kaufman, H.L., Collichio, F., Amatruda, T., Senzer, N., Chesney, J., Delman, K.A., Spitler, L.E., Puzanov, I., Agarwala, S.S., et al. (2015). Talimogene laherparepvec improves durable response rate in patients with advanced melanoma. J. Clin. Oncol. *33*, 2780–2788.
18. Zhang, Y., Li, Y., Chen, K., Qian, L., and Wang, P. (2021). Oncolytic virotherapy reverses the immunosuppressive tumor microenvironment and its potential in combination with immunotherapy. Cancer Cell Int *21*, 262.
19. Zheng, M., Huang, J., Tong, A., and Yang, H. (2019). Oncolytic viruses for cancer therapy: barriers and recent advances. Mol. Ther. oncolytics *15*, 234–247.
20. Pipiya, T., Sauthoff, H., Huang, Y.Q., Chang, B., Cheng, J., Heitner, S., Chen, S., Rom, W.N., and Hay, J.G. (2005). Hypoxia reduces adenoviral replication in cancer cells by downregulation of viral protein expression. Gene Ther. *12*, 911–917.
21. Zhou, Y., Wen, F., Zhang, P., Tang, R., and Li, Q. (2016). Vesicular stomatitis virus is a potent agent for the treatment of malignant ascites. Oncol. Rep. *35*, 1573–1581.
22. Ishikawa, W., Kikuchi, S., Ogawa, T., Tabuchi, M., Tazawa, H., Kuroda, S., Noma, K., Nishizaki, M., Kagawa, S., Urata, Y., and Fujiwara, T. (2020). Boosting replication and penetration of oncolytic adenovirus by paclitaxel eradicate peritoneal metastasis of gastric cancer. Mol. Ther. oncolytics *18*, 262–271.
23. Lauer, U.M., Schell, M., Beil, J., Berchtold, S., Koppenhöfer, U., Glatzle, J., Königsrainer, A., Möhle, R., Nann, D., Fend, F., et al. (2018). Phase I study of oncolytic vaccinia virus GL-ONC1 in patients with peritoneal carcinomatosis. Clin. Cancer Res. *24*, 4388–4398.
24. Liang, M. (2018). Oncorine, the world first oncolytic virus medicine and its update in China. Curr. Cancer Drug Targets *18*, 171–176.

25. Bischoff, J.R., Kirn, D.H., Williams, A., Heise, C., Horn, S., Muna, M., Ng, L., Nye, J.A., Sampson-Johannes, A., Fattaey, A., and McCormick, F. (1996). An adenovirus mutant that replicates selectively in p53-deficient human tumor cells. Science *274*, 373–376.

26. Lu, W., Zheng, S., Li, X.F., Huang, J.J., Zheng, X., and Li, Z. (2004). Intra-tumor injection of H101, a recombinant adenovirus, in combination with chemotherapy in patients with advanced cancers: a pilot phase II clinical trial. World J. Gastroenterol. *10*, 3634–3638.

27. Xia, Z.J., Chang, J.H., Zhang, L., Jiang, W.Q., Guan, Z.Z., Liu, J.W., Zhang, Y., Hu, X.H., Wu, G.H., Wang, H.Q., et al. (2004). [Phase III randomized clinical trial of intratumoral injection of E1B gene-deleted adenovirus (H101) combined with cisplatin-based chemotherapy in treating squamous cell cancer of head and neck or esophagus]. Ai Zheng *23*, 1666–1670.

28. Garber, K. (2006). China approves world's first oncolytic virus therapy for cancer treatment. J. Natl. Cancer Inst. *98*, 298–300.

29. Lei, J., Li, Q.H., Yang, J.L., Liu, F., Wang, L., Xu, W.M., and Zhao, W.X. (2015). The antitumor effects of oncolytic adenovirus H101 against lung cancer. Int. J. Oncol. *47*, 555–562.

30. Li, Y., He, J., Qiu, C., Shang, Q., Qian, G., Fan, X., Ge, S., and Jia, R. (2019). The oncolytic virus H101 combined with GNAQ siRNA-mediated knockdown reduces uveal melanoma cell viability. J. Cell Biochem. *120*, 5766–5776.

31. He, C.B., Lao, X.M., and Lin, X.J. (2017). Transarterial chemoembolization combined with recombinant human adenovirus type 5 H101 prolongs overall survival of patients with intermediate to advanced hepatocellular carcinoma: a prognostic nomogram study. Chin J. Cancer *36*, 59.

32. Overgaard, N.H., Jung, J.W., Steptoe, R.J., and Wells, J.W. (2015). CD4+/CD8+ double-positive T cells: more than just a developmental stage? J. Leukoc. Biol. *97*, 31–38.

33. D'Acquisto, F., and Crompton, T. (2011). CD3+CD4-CD8- (double negative) T cells: saviours or villains of the immune response? Biochem. Pharmacol. *82*, 333–340.

34. Ayantunde, A.A., and Parsons, S.L. (2007). Pattern and prognostic factors in patients with malignant ascites: a retrospective study. Ann. Oncol. *18*, 945–949.

35. Becker, G., Galandi, D., and Blum, H.E. (2006). Malignant ascites: systematic review and guideline for treatment. Eur. J. Cancer *42*, 589–597.

36. Hodge, C., and Badgwell, B.D. (2019). Palliation of malignant ascites. J. Surg. Oncol. *120*, 67–73.

37. Zhao, H., Xu, C., Luo, X., Wei, F., Wang, N., Shi, H., and Ren, X. (2018). Seroprevalence of neutralizing antibodies against human adenovirus type-5 and chimpanzee adenovirus type-68 in cancer patients. Front Immunol. *9*, 335.

38. Rivadeneira, D.B., DePeaux, K., Wang, Y., Kulkarni, A., Tabib, T., Menk, A.V., Sampath, P., Lafyatis, R., Ferris, R.L., Sarkar, S.N., et al. (2019). Oncolytic viruses engineered to enforce leptin expression reprogram tumor-infiltrating T cell metabolism and promote tumor clearance. Immunity *51*, 548–560.e4.

39. Lowther, D.E., Goods, B.A., Lucca, L.E., Lerner, B.A., Raddassi, K., van Dijk, D., Hernandez, A.L., Duan, X., Gunel, M., Coric, V., et al. (2016). PD-1 marks dysfunctional regulatory T cells in malignant gliomas. JCI Insight *1*, e85935.

40. Park, H.J., Park, J.S., Jeong, Y.H., Son, J., Ban, Y.H., Lee, B.H., Chen, L., Chang, J., Chung, D.H., Choi, I., and Ha, S.J. (2015). PD-1 upregulated on regulatory T cells during chronic virus infection enhances the suppression of CD8+ T cell immune response via the interaction with PD-L1 expressed on CD8+ T cells. J. Immunol. *194*, 5801–5811.

41. Mayoux, M., Roller, A., Pulko, V., Sammicheli, S., Chen, S., Sum, E., Jost, C., Fransen, M.F., Buser, R.B., Kowanetz, M., et al. (2020). Dendritic cells dictate responses to PD-L1 blockade cancer immunotherapy. Sci. Transl Med. *12*, eaav7431.

42. Ando, K., Hamada, K., Shida, M., Ohkuma, R., Kubota, Y., Horiike, A., Matsui, H., Ishiguro, T., Hirasawa, Y., Ariizumi, H., et al. (2021). A high number of PD-L1(+) CD14(+) monocytes in peripheral blood is correlated with shorter survival in patients receiving immune checkpoint inhibitors. Cancer Immunol. Immunother. *70*, 337–348.

43. Inadomi, J., Cello, J.P., and Koch, J. (1996). Ultrasonographic determination of ascitic volume. Hepatology *24*, 549–551.

44. Oh, S.Y., Kwon, H.C., Lee, S., Lee, D.M., Yoo, H.S., Kim, S.H., Jang, J.S., Kim, M.C., Jeong, J.S., and Kim, H.J. (2007). A Phase II study of oxaliplatin with low-dose leucovorin and bolus and continuous infusion 5-fluorouracil (modified FOLFOX-4) for gastric cancer patients with malignant ascites. Jpn. J. Clin. Oncol. *37*, 930–935.